J. COMBIN. MATH. COMBIN. COMPUT. 127b (2025) 3051--3072

Journal of Combinatorial Mathematics
and Combinatorial Computing
www.combinatorialpress.com/jcmcc

Research on cooperative scheduling and power restoration strategy of intelligent operation and maintenance equipment under flood disaster based on dynamic planning

Hao Dai[1], Guowei Liu[1,✉], Lisheng Xin[1], Longlong Shang[1], Qingmiao Guo[1], Hao Deng[1]

[1] *Shenzhen Power Supply Co., Ltd., Shenzhen, Guangdong, 518000, China*

ABSTRACT

In order to cope with the damage of urban electricity and the dilemma of residents' electricity consumption caused by flooding disaster, we study the dynamic planning of intelligent operation and maintenance equipment scheduling and distribution network restoration under flooding disaster. Consideration is given to both pre-disaster deployment and post-disaster scheduling levels, while dynamic planning is carried out for collaborative repair and energy storage scheduling to construct a scheduling model with multi-source collaboration. Based on this, a multi-resource cooperative post-disaster recovery strategy for distribution networks is further proposed. The usability of this paper's multi-source cooperative strategy is studied in depth through case analysis. Among the six Cases of the simulation experiment, the total cost in Case 1, which is operated and restored according to the strategy proposed in this paper, is the lowest, which is only 257080.2 RMB. The maximum, minimum, and average values of the solution time of the multi-source cooperative strategy are much faster than those of the comparison methods, and it has obvious advantages in fast decision making. The multi-source synergy model in this paper is able to recover all the loads within 285 min, while the finite synergy model takes 330 min. The multi-source synergy model was able to recover 7,500 kW of load, while the limited synergy model was only able to recover 6,850 kW. The multi-source cooperative model has strong applicability.

Keywords: dynamic planning, cooperative scheduling, multi-source collaboration, intelligent operation and maintenance equipment, power restoration

1. Introduction

Flooding is a natural disaster in which the depth of water on the ground in urban or rural areas exceeds normal due to excessive precipitation, poor drainage, topography, urban planning and other reasons, resulting in serious obstruction of urban or rural transportation, production, and housing [1]. Once

✉ Corresponding author.
E-mail address: LiuGuowei202401@163.com (G. Liu).
Received 20 December 2024; Revised 05 February 2025; Accepted 25 March 2025; Published Online 16 April 2025.
DOI: 10.61091/jcmcc127b-171

the flooding situation occurs, it is necessary to quickly take effective disposal measures to reduce losses and protect people's lives and property.

In recent years, with the development of the communication system, carrying the production, control and management of a variety of business volume of rapid growth, the distribution network on its dependence on the increasing, and the frequent occurrence of disasters so that the distribution network blackout, power system paralysis, and other risks are increasing, the power system and the distribution network communication system restoration of the disaster situation is essential to understand and disaster relief [2-4]. The first step in a large-scale failure of the power system after a disaster is to conduct a disaster assessment and determine the urgency of power supply restoration [5]. Disaster assessment provides the extent of damage caused by the disaster, damage to power facilities, and the resources and time required for restoration [6-7]. At the same time, emergency power sources and backup grids are activated to protect the power supply needs of critical equipment and important power users, and to ensure the basic power needs of the society, while the damaged power equipment is then quickly repaired and power facilities such as transformers, transmission lines, and power supply equipment are overhauled [8-11]. This process involves collaboration among government departments, power repairers, road repairers, and other personnel, as well as the development of repair strategies, mobilization of staff and equipment resource allocation, and other complexities [12-14]. In disaster and post-disaster relief, the deployment of equipment is a crucial part, only rational planning and scheduling, in order to better cope with the disaster, to protect people's lives and property safety. The general deployment principle is based on the demand and disaster level, both of which change in real time in the actual situation, and it is difficult to generate the dispatching program of its equipment quickly. And intelligent operation and maintenance through artificial intelligence, big data, cloud computing and other technologies, to achieve automation, intelligent management, and reduce the time and cost of manual intervention to quickly give a reasonable solution [15-16]. Therefore, it has become a new research direction to cope with the collaborative scheduling of equipment and power restoration in the disaster environment by means of intelligent operation and maintenance.

The article considers the flood disaster repair and post-disaster energy storage scheduling to construct an emergency restoration resource scheduling model and a distribution network operation model. At the same time, it constructs a multi-resource cooperative scheduling model from both pre-disaster deployment and post-disaster scheduling. Then, in-depth exploration is carried out for post-disaster distribution network recovery, and a multi-source cooperative post-disaster recovery strategy for distribution networks is proposed. An example analysis is conducted to verify the feasibility of the multisource cooperative scheduling and distribution network restoration strategy proposed in this paper. Meanwhile, the load restoration and total cost of the distribution network with the multi-source cooperative strategy of this paper are obtained. The load restoration results and distribution network topology results after the flooding disaster are analyzed. Finally, it is compared with the finite synergy model to verify its applicability.

2. Overview

In terms of transportation equipment scheduling, literature [17] responded to the flood disaster by constructing a helicopter aviation emergency rescue scheduling model and a multi-agent helicopter aviation emergency rescue scheduling simulation system, which not only involves the basic mission requirements and starting points, but also covers the whole scheduling factors including the properties of the helicopter itself, command center, loading and unloading locations, and material placement points. Literature [18] designed a vehicle scheduling and path planning model for emergency supplies under multiple dynamics and objectives, which can consider maximizing vehicle transportation efficiency and minimizing the difference in emergency response level in the changing disaster situation, and transport multiple emergency supplies stockpile points to different disaster points. In terms of medical equipment scheduling, literature [19] utilized a self-constructed evaluation system for the degree of emergency demand for emergency medical equipment and established a model for the distribution of urban emergency medical equipment based on the degree of emergency of the demand, time, and vehicle loading, which also possesses the functions of reducing the distribution cost and planning the optimal routes for distribution. Similarly, in considering the degree of disaster emergency and medical demand, literature [20] gives a large-scale emergency medical material scheduling algorithm through heterogeneous ant colony algorithm and reinforcement learning, which not only improves the scheduling efficiency, but also solves the problem of fairness of medical distribution in multiple disaster sites.

In the study of post-disaster power restoration, literature [21] developed a post-disaster power system restoration planning model based on the sequential correlation restoration cycle, which takes the minimization of restoration duration and the maximization of power system load capacity as the key. Literature [22] utilized an intentional islanding algorithm for post-disaster power supply restoration based on restoring power strategies to distributed energy resources. Literature [23] customized and developed optimal recovery plans and heuristic algorithms for power restoration strategies in disaster environments, respectively, with the former having better restoration strength and better life safety assurance for maintenance personnel. Literature [24] obtains electric vehicle characteristics with travel chains and probability distribution functions, and develops a post-disaster distribution network power restoration model in this context, which solves the load problem in post-disaster distribution network restoration. Literature [25] constructs a multiple cooperative distribution network emergency repair allocation model to solve the optimal allocation restoration strategy under cooperative cooperation with dynamic planning, which solves the delay problem in the process of distribution network restoration.

3. A unified model for pre-disaster deployment and post-disaster scheduling of flooding disasters

In this chapter, considering the operational characteristics of the drainage team, maintenance team coordinated repair scheduling and mobile energy storage scheduling, a multi-resource coordinated emergency restoration resource scheduling model is constructed, and a multi-resource coordinated pre-disaster deployment and post-disaster scheduling unified model is established by combining the transferring role of the remote switches as well as the safe operation constraints of the distribution network.

3.1. Emergency recovery resource mobilization model

3.1.1. Repair scheduling model. The repair scheduling process can be modeled as a multilogistics center vehicle path planning problem, the proposed model takes into full consideration of the same type of repair team repair and different repair team timing with the relationship.

1) Spatial constraints of repair scheduling:

$$\sum_{n \in C_{n,r}} D_{ep,g,n} \le 1 \quad \forall g \in P \cup F \tag{1}$$

$$\sum_{m \in C_{n,r}} x_{n,g,m,s} \le D_{ep,g,n} \quad \forall n \in C_{sp}, \forall s \in S, \forall g \tag{2}$$

$$\sum_{m \in C_{n,r} \cup C_{n,r}} x_{n,g,m,s} - \sum_{m \in C_{n,r} \cup C_{n,r}} x_{m,g,n,s} = 0 \;\; \forall n \in C_{D,s}, \forall g, \forall s \tag{3}$$

$$\sum_{m \in C_{1,\dots} \cup C_{np}} x_{m,g,n,s} \le 1 \quad \forall n \in C_{n,s}, \forall g, \forall s \tag{4}$$

$$\sum_{m\in C_{0,\ldots}\cup C_w} x_{m,g,n,s} = 1 \quad \forall n \in C_{DP}, \forall g, \forall s \tag{5}$$

$$y_{n,g,s} = \sum_{m\in C_{D,s}\cup C_{D,s}} x_{n,g,m,s} \quad \forall n \in C_{D,s}, \forall g, \forall s \tag{6}$$

$$\sum_{g\in P\cup F} y_{n,g,s} \le K_n \quad \forall n \in C_{D.s}, \forall s \tag{7}$$

where C_{sp}, C_{pp} is the start and end point collection of repair teams, i.e., the collection of emergency warehouse locations, respectively. $D_{ep.g.n}$ is the pre-disaster deployment location 0-1 variable, and $D_{cp.g.n} = 1$ indicates that the repair team g is deployed in the emergency warehouse n. P, F is the collection of drainage and maintenance teams, respectively. S is the set of generated post-disaster failure scenarios. C_D is the set of faulty components under scenario s, including flooded components and damaged components. $x_n.g.m.s$ is the post-disaster scheduling strategy 0-1 variable, $x_{n,g,m,s} = 1$ indicating that the repair team g under scenario s is dispatched from the faulty element (or starting point) n to the faulty element (or end point) m. $y_n.g.s$ is the 0-1 variable, $y_{n.g,s} = 1$ indicating that the repair team g under scenario s has arrived at the faulty element n, and vice versa. K_n is the maximum number of salvage teams involved in the faulty element n repair.

Eq. (1) is the repair team deployment constraint, which indicates that each repair team can only be deployed in one emergency warehouse. Eq. (2) indicates that the repair team can only depart from its deployment location. Eq. (3) is the personnel flow conservation constraint. Eq. (4) indicates that repair teams do not arrive at the same element repeatedly. Eq. (5) indicates that all repair teams must return to the end point after completing their tasks. Eq. (6) indicates that if an element exists in the scheduling path of a repair team, the team has reached that element. Equation (7) limits the number of teams involved in repairing the same component.

2) Repair scheduling time constraint:

$$0 \le t_{rch,n,g,s} - \sum_{m\in C_{sr}} x_{m,g,n,s} t_{travel,m,g,n} \le \left(1 - \sum_{m\in C_{sx}} x_{m,g,n,s}\right) M \quad \forall n \in C_{D.s}, \forall g, \forall s \tag{8}$$

$$t_{bgn,n,g,s} \ge t_{rch,n,g,s} \quad \forall n \in C_{D,s}, \forall g, \forall s \tag{9}$$

$$\begin{gathered} t_{bgn,n,g,s} + t_{cnsm,n,g,s} + t_{travel,n,g,m} - t_{rch,m,g,s} \le (1 - x_{n,g,m,s}) M \\ \forall n \in C_{D.s}, m \in C_{D.s} \cup C_{DP}, \forall g, \forall s \end{gathered} \tag{10}$$

where $t_{rch,n,g,s}$ is the moment when the emergency repair team g arrives at the faulty element n under scenario s. $t_{travel.m.g.n}$ is the travel time of the repair team g from the faulty element (or starting point) m to the faulty element (or end point) n. M is a large positive real number. $t_{bgn,n.g.s}$ is the moment when the repair team g starts repairing the faulty element n under scenario s. $t_{cnsm.n.g.s}$ is the operating time of the repair team g at the faulty element n under scenario s.

Equation (8) indicates that when the faulty element n is the 1st arrival position of the repair team g, the arrival moment shall be the traffic time from the starting point to the element n. Equation (9) indicates that the moment when the repair team starts operation at the faulty element is not less than the arrival moment. Equation (10) indicates that the repair team can arrive at more than one component, and the arrival moment is not less than the sum of the start of operation moment, operation time and traffic time at the previous faulty component.

3) Resource constraints for repair scheduling:

$$\sum_{n\in C_{w,s}} C_{cap,n,p,s} \le C_{cap,max,p} \quad \forall p\in P,\forall s \tag{11}$$

$$0\le c_{cap,n,p,s} \le y_{n,p,s} c_{cap,dem,n,s} \quad \forall n\in C_{w,s},\forall p,\forall s \tag{12}$$

$$\sum C_{cap,n,p,s} = C_{cap,dem,n,s} \quad \forall n\in C_{W.s},\forall s \tag{13}$$

$$\sum_{n\in C_{n,s}} c_{res,n,f,s} \le c_{res,\max,f} \quad \forall f\in F,\forall s \tag{14}$$

$$0\le c_{res,n,f,s} \le y_{n,f,s} c_{res,dem,n,s} \quad \forall n\in C_{B,s},\forall f,\forall s \tag{15}$$

$$\sum_{j\in F} c_{res,n,f,s} = c_{res,dem,n,s} \quad \forall n\in C_{B,s},\forall s \tag{16}$$

where $C_{W,s}, C_{B,s}$ is the set of flooded and damaged elements under scenario s, respectively. $c_{cap,n,p,s}$ is the discharge of drainage team p at flooded element n under scenario s. $c_{cap,max.p}$ is the maximum drainage volume of drainage team ρ. $c_{cap,dem,n,s}$ is the amount of water to be drained at flooded element n under scenario s. $c_{res,n,f,s}$ is the maintenance resource consumption of maintenance team f at damaged element n under scenario s. $c_{res.max.f}$ is the amount of repair resources carried by repair team f. $c_{res,dem,n.s}$ is the repair resource requirement at damaged element n under scenario s.

Eq. (11) indicates that each dewatering team may not exceed its maximum dewatering capacity, which is generally limited by pump power capacity. Equation (12) indicates that only the drainage teams that have reached the flooded element n may participate in the drainage of that element. Equation (13) indicates that the total volume of water discharged at Element n by each drainage team participating in the dewatering of Flooded Element n shall be equal to the volume of water to be discharged at Element n. Eq. (14) indicates that each maintenance team has a limited capacity for transporting supplies, and that the maintenance resources consumed during the maintenance process must not exceed its maximum supply carrying capacity. Eq. (15) indicates that only the repair team that has arrived at damaged element n may participate in the repair of that element. Equation (16) indicates that the total resources invested in component n by the repair teams participating in the repair of component n should be equal to the amount of resources required to repair component n.

4) Collaborative repair process constraints:

$$t_{cnsm,n,p,s} = \frac{C_{cap,n,p,s}}{q_P} \forall n\in C_{w,s},\forall p,\forall s \tag{17}$$

$$0\le t_{cnsm,n,f,s} \le y_{n,r,s} M \forall n\in C_{B,s},\forall f,\forall s \tag{18}$$

$$\sum_{f\in F} \frac{t_{cnsm,n,f,s}}{t_{rqr,n,f,s}} \ge 1 \forall n\in C_{B,s},\forall s \tag{19}$$

$$\sum_{t\in T} td_{n,t,s} \ge t_{bgn,n,p,s} + t_{cnsm,n,p,s} \quad \forall n\in C_{W,s},\forall p,\forall s \tag{20}$$

$$\sum_{t\in T} th_{n,t,s} \ge t_{bgn,n,f,s} + t_{cnsm,n,f,s} \quad \forall n\in C_{B,s},\forall f,\forall s \tag{21}$$

$$t_{bgn,n,f,s} \ge \sum_{t\in T} td_{n,t,s} \quad \forall n\in C_{W,s}\cap C_{B,s},\forall f,\forall s \tag{22}$$

$$\sum_{t\in T} d_{n.t.s} \le 1 \quad \forall n\in C_{\mathrm{w.s}},\forall s \tag{23}$$

$$\sum_{t\in T} h_{n,t,s} \le 1 \quad \forall n \in C_{\mathrm{B}.s}, \forall s \tag{24}$$

$$\rho_{n,t,s} \le \sum_{t=0}^{t} d_{n,t,s} \quad \forall n \in C_{\mathrm{W}.s}, \forall t \in T, \forall s \tag{25}$$

$$\rho_{n,t,s} \le \sum_{t=0}^{t} h_{n,t,s} \quad \forall n \in C_{\mathrm{B}.s}, \forall t, \forall s \tag{26}$$

where q_ρ is the rate of drainage of drainage team p. $t_{rqr.n.f,s}$ is the scenario s the lower repair team f the time required to repair damaged elements n individually. T is the set of recovery time periods. $d_{n.t.s}$ is a 0-1 variable, $d_{n.t.s} = 1$ means that the water at the flooded element n under scenario s is drained at the moment t. $h_{n.t.s}$ is a 0-1 variable that $h_{n.t.s} = 1$ indicates that the damaged element n under scene s is repaired at moment t. $\rho_{n.t.s}$ is a 0-1 variable indicating the energized state of element n at moment t under scene s.

Equation (17) indicates that the time that the drainage team spends at the flooded element is proportional to the amount of water discharged. Equation (18) indicates that only the repair team that has reached damaged element n can participate in the repair of that element. Unlike the drainage process, the repair operation time consumed is not directly related to the amount of maintenance resources consumed. Therefore, the repair process of the damaged element is described by Eq. (19), i.e., when only one repair team is involved in the repair, the operation time shall be the time required by the repair team to repair the damaged element alone. When multiple repair teams collaborate in the repair, the repair progress of repair team f is denoted by $t_{cnsm,n,f,s} / t_{rqr,n,f,s}$. Component n is repaired when the sum of the progress of the repair teams involved in the repair of damaged component n is 1.

3.1.2. Mobile Energy Storage Dispatch Models. Mobile energy storage is a commonly used movable power source [26-27], with temporal and spatial flexibility in power generation, which can be used as a distributed power source for emergency power support to isolated islands. In this paper, mobile energy storage deployment and dispatch are incorporated into a cooperative scheduling model, which cooperates with the emergency repair process to realize rapid post-disaster load recovery. Mobile energy storage dispatching needs to satisfy spatio-temporal constraints and operational constraints. The following are the spatio-temporal constraints of mobile energy storage:

$$\sum_{n\in C_{sr}} D_{ep.e.n} \le 1 \forall e \in M_{ESS} \tag{27}$$

$$\sum_{i\in N} x_{n,e,i,s} \le D_{ep,e,n} \quad \forall n \in C_{SP}, \forall e, \forall s \tag{28}$$

$$y_{E,i,e,s} = \sum_{n\in C_{sx}} x_{n,e,i,s} \quad \forall i \in N, \forall e, \forall s \tag{29}$$

$$0,, t_{rch,i,e,s} - \sum_{n\in C_{sr}} x_{n,e,i,s} t_{travel,n,g,i} \le \left(1 - \sum_{n\in C_{sr}} x_{n,e,i,s}\right) M \quad \forall i, \forall e, \forall s \tag{30}$$

$$\sum_{t\in T} t k_{i,e,t,s} \ge t_{rch,i,e,s} \quad \forall i, \forall e, \forall s \tag{31}$$

$$\sum_{t\in T} k_{i,e,t,s} \le y_{E.i,e,s} \quad \forall i, \forall e, \forall s \tag{32}$$

$$\rho_{E,i,e,t,s} \le \sum_{t=0}^{t} k_{i,e,t,s} \quad \forall i, \forall e, \forall t, \forall s \tag{33}$$

$$\rho_{E,i,e,t,s} \le \sum_{t=0}^{t} d_{i,t,s} \quad \forall i, \forall e, \forall t, \forall s \tag{34}$$

where, $D_{ep,e.n}$ is the pre-disaster deployment location 0-1 variable, $D_{ep,e.n}=1$ denotes that the mobile energy storage e is deployed in the emergency warehouse n. M_{ESS} is the mobile energy storage collection. N is the set of distribution network nodes. $y_{E.i.e.s}$ is a 0-1 variable, $y_{E.i.e.s}=1$ denotes that the target node of mobile storage energy e under scenario s is node i. $k_{i,e,t,s}$ is a 0-1 variable, $k_{i,e,t,s}=1$ denotes that the mobile storage energy e under scenario s reaches the target node i at the tth moment. $\rho_{E.i,e.ts}$ is a 0-1 variable denoting that the mobile storage energy e under scenario s operates at node i at the tth moment.

3.2. Distribution network operation model

The pre-disaster deployment and post-disaster recovery model considers the role of remote switching for transferring supply and the recovery process needs to meet the actual operational requirements of the distribution grid. The following topological constraints for distribution network operation are presented:

$$\sum_{t\in T} \beta_{ij,t,s} \le \beta_{\max,ij} \forall ij \in L, \forall s \tag{35}$$

$$\beta_{ij,t,s} \ge \rho_{ij,t,s} - \rho_{ij,t-1,s} \forall ij, \forall t, \forall s \tag{36}$$

$$\beta_{ij,t,s} \ge \rho_{ij,t-1,s} - \rho_{ij,t,s} \forall ij, \forall t, \forall s \tag{37}$$

$$\rho_{+,ij,t,s} + \rho_{-,ij,t,s} = \rho_{ij,t,s} \forall ij, \forall t, \forall s \tag{38}$$

$$\sum_{k:(k,i)\in L} \rho_{+,ki,t,s} + \sum_{j:(i,j)\in L} \rho_{-,ij,t,s} \le \frac{|N|-|G|}{|N|-|G|+1} \forall i \in N \setminus G, \forall t, \forall s \tag{39}$$

$$\sum_{i\in G}\left(\sum_{k:(k,i)\in L} \rho_{+,ki,t,s} + \sum_{j:(i,j)\in L} \rho_{-,ij,t,s} \right) \le \frac{|N|-|G|}{|N|-|G|+1} \forall t, \forall s \tag{40}$$

$$\rho_{+,ij,t,s}, \rho_{-,ij,t,s} \ge 0 \quad \forall ij, \forall t, \forall s \tag{41}$$

where L is the set of distribution network lines. $\beta_{ij,t.s}$ is the switch action 0-1 variable, and $\beta_{ij,t,s}=1$ denotes the scenario s under which the state of the remote switch on the line ij changes at the t moment. $\rho_{ij,t,s}$ is the line connectivity state 0-1 variable. $\rho_{+.ij,t,s}\rho_{-.ij,t,s}$ is the continuous auxiliary variable. G is the set of substation nodes. $|N|,|G|$ is the number of nodes and substations in the distribution network, respectively.

3.3. Pre-disaster deployment model

The optimization objective of the pre-disaster deployment model in this paper is to maximize the load recovery expectation under various possible disaster scenarios:

$$\max \sum_{s\in S} \pi_s \sum_{t\in T} \sum_{i\in N} w_i \rho_{\text{load},i,t,s} p_{\text{load},i,t} \Delta t \tag{42}$$

where π_s is the occurrence probability of scenario s. w_i is the weight factor of the load at node i, which indicates the importance of the load.

3.4. *Post-disaster dispatch model*

The optimization objective of the post-disaster scheduling model is to maximize the post-disaster load recovery of the distribution network under a defined disaster scenario and deployment plan:

$$\max \sum_{t \in T} \sum_{i \in N} w_i \rho_{\text{load},i,t,s_0} p_{\text{load},i,t} \Delta t \tag{43}$$

where s_D is a determined post-disaster fault scenario that can be generated by post-disaster situational awareness.

Taking Eq. (43) as the objective function, the post-disaster fault scenario is substituted into the constraints Eq. (1) to Eq. (41) to construct the mixed-integer second-order cone planning model for post-disaster scheduling (MISOCP).

4. Multi-source synergistic post-disaster recovery strategy for distribution networks

4.1. *Objective function*

In this paper, we establish a coordinated optimal dispatch model for post-disaster power supply restoration with the objective of maximizing the overall benefits of the distribution grid side and EVA after an inland flooding disaster as a means of determining the on/off decision of the distribution grid branch, the time transfer and energy dispatch scheme of the MES, the amount of power traded between the EVA and the distribution grid as well as the size of the additional incentive price signals to be released to the EV users. The objective function of this paper can be expressed as:

$$F = \max\left(-F_1 + F_2\right) \tag{44}$$

F_1 is the loss due to power outages on the distribution side, see equation (45). The term 1 in F_1 represents the losses from outages for all types of industrial users. In order to avoid wasting emergency resources, the terms representing the dispatch costs for emergency restoration of energy are added to F_1. They point to the cost of power purchased by EVA, the cost of moving and charging MES, and the cost of DSG and WG outages, respectively:

$$\begin{aligned} F_1 = \sum_{t=1}^{T} \Bigg[& \sum_{z \in S_{ind}} \sum_{j \in S_t} l_z \left(1 - \alpha_{j,t}\right) P_{j,t}^{D} + \sum_{n \in S_{EN}} C_{ac} P_{n,t}^{EV} + \\ & \sum_{m \in S_{MES}} \left(C_m \sum_{r' \to r \in \Omega_g} \lambda_{r' \to r,t}^{m} + \sum_{r \in R} C_p P_{m,r,t}^{cha} \right) \\ & + \sum_{w \in S_{BC}} C_g P_{w,t}^{DSG} + \sum_{f \in S_{BC}} C_W P_{f,t}^{W} \Bigg] \Delta T + \sum_{m \in S_{MES}} C_p E_m^{MES} \end{aligned} \tag{45}$$

where, S_{ind} is the set of categories of user classification. S_z is the set of subordinate category z industry power nodes. l_z is the unit cut load loss of industry unit of category z. $\alpha_{j,t}$ is the decision variable for the load recovery state at node j in time period t, with a load recovery time value of 1. $P_{j,t}$ is the active power demand of the load at node j in time period t. S_{EV} is the set of EV charging sites. C_{ac} is the unit subsidized tariff paid by the grid to the EVA. S_{MES} is the set of MES. C_m is the unit time traveling cost of the MES. $P_{m,r,t}^{cha}$ is the charging power of the m th MES access point r in time t. C_p is the unit charging cost of the MES. S_{bsc} is the aggregation of DSGs. C_g is the output cost per unit of power generated by the DSG. $P_{w,t}^{DSG}$ is the active power out of the w th DSG in t time period. S_{WG} is the set of WGs. C_w is the unit generation cost of WG. $P_{f,t}^{w}$ is the predicted active output of the f th WG in the t time period E_m^{MES} is the battery capacity of the m nd MES.

F_2 is the EVA side revenue, which comes from the difference between the revenue from selling electricity to the grid side and the cost paid to the EV users for their discharge response behavior, and can be expressed as:

$$F_2 = \sum_{i=1}^{T} \sum_{n \in S_{EX}} \left[C_{ac} - \left(\frac{C_{EV}}{\eta_n^2} + x_{1,n} \right) \right] P_{n,t}^{EV} \Delta T \tag{46}$$

where C_{EV} is the unit charging cost of the EV, $\frac{C_{EV}}{\eta_n^2}$ is the base tariff paid by the EVA to the EV after taking into account the charging and discharging efficiencies. $x_{1,n}$ is the additional incentive tariff paid by EVA.

4.2. Constraints

4.2.1. Radial topology constraints for distribution networks. In order to fully utilize the fault resilience of distributed generating units (DGs) including DSGs and WGs, this paper employs an improved single-commodity flow method to ensure the radial-like requirement of the distribution network topology. The root node state decision variable is introduced, the reconfigured number of islands is added to the optimization process, and the Big-M method is applied to relax the virtual currents as follows:

$$\sum_{i-j \in S_1} \omega_{i-j,t} = N^n - \sum_{i \in S_{nC}} \gamma_{i,t} \tag{47}$$

$$\sum_{i \in S_s(j)} R_{ij,t} = \sum_{h \in S_{sa}(j)} R_{j-h,t} + D_j \quad j \in S_N \setminus S_{pG} \tag{48}$$

$$R_j^{VS} + \sum_{i \in S_{in}(j)} R_{ij,t} = \sum_{h \in S_{int}(j)} R_{j \cdot h,t} + D_j \quad j \in S_{DG} \tag{49}$$

$$-M\gamma_{j,t} \le R_j^{VS} \le M\gamma_{j,t} \quad j \in S_{DG} \tag{50}$$

$$-M\,\omega_{i \cdot j,t} \le R_{i \cdot j,t} \le M\,\omega_{i \cdot j,t} \tag{51}$$

$$\omega_{ij,t} \le S_{ij,t} \tag{52}$$

where S_{bc} is the set of nodes where DSG and WG are located. S_L is the set of distribution network tributaries. $\omega_{i,j,t}$ is a decision variable indicating the connectivity status of branch $i-j$ in time period t, with a value of 1 when the branch is connected. N^n is the total number of nodes within the distribution network. $\gamma_{n,t}$ is a decision variable indicating whether the v th DG acts as the root node of the silo in which it is located. $S_{in}(j), S_{out}(j)$ are the sets of upstream and downstream nodes of node j, respectively. $R_{i,j,t}, R_{j,h,t}$ are the virtual currents flowing through branch $i-j, j-h$ during time t, respectively. D_j is the virtual load demand at node j. $S_N \setminus S_{DG}$ is the set of nodes in the distribution network except at DG. R_j^{vs} is the virtual power emitted at node j. M is a sufficiently large positive number. $S_{ij,t}$ is the power dispatch center's predicted t time period branch circuit $i-j$ restoration status.

Eq. (47) represents the relationship between the branch opening and disconnecting states and the number of nodes and islands in the distribution network, where for each additional island, one more branch is disconnected to satisfy the radial constraints of the distribution network topology. Eq. (48) and Eq. (49) represent the virtual power balance relationship at the root node and non-root node, respectively. Eq. (50) and Eq. (51) are the virtual root node outgoing power and virtual tidal flow through constraints, respectively. Eq. (52) indicates that the branch remains disconnected until it is repaired.

4.2.2. MES energy constraints. The MES takes the energy storage battery as a carrier and obeys the scheduling instruction to go to the target access point to complete the charging and discharging work to realize the energy transfer within the distribution network.The energy model of the MES is expressed as follows:

$$0 \le \sum_{r \in R} P_{m,r,t}^{dis} \le \varepsilon_{m,t}^{dis} P_{m,\max}^{dis} \tag{53}$$

$$0 \le P_{m,r,t}^{cha} \le \mu_{r,t}^{m} P_{m,\max}^{cha} \tag{54}$$

$$0 \le \sum_{r \in R} P_{m,r,t}^{dis} \le \varepsilon_{m,t}^{dis} P_{m,\max}^{dis} \tag{55}$$

$$0 \le \sum_{r \in R} P_{m,r,t}^{cha} \le \varepsilon_{m,t}^{cha} P_{m,\max}^{cha} \tag{56}$$

$$\varepsilon_{m,t}^{dis} + \varepsilon_{m,t}^{cha} \le \sum_{r \in R} \mu_{r,t}^{m} \tag{57}$$

$$S_{m,t+1}^{SOC} == S_{m,t}^{SOC} + \left(\eta_m \sum_{r \in R} P_{m,r,t}^{cha} - \frac{\sum_{r \in R} P_{m,r,t}^{dis}}{\eta_m} \right) \frac{\Delta T}{E_m^{MES}} \tag{58}$$

$$S_{m,\min}^{SOC} \le S_{m,t}^{SOC} \le S_{m,\max}^{SOC} \tag{59}$$

where $P_{m,r,t}^{dis}$ is the discharging power of the m rd MES access point r in time t. $P_{m,\max}^{cha}$ and $P_{m,\max}^{dis}$ are the upper limit of the charging and discharging power of the m th MES, respectively. $\varepsilon_{m,t}^{cha}$ and $\varepsilon_{m,t}^{dis}$ are the charging and discharging states of the m th MES, respectively. η_m is the charging and discharging efficiency of the m th MES. $S_{m,t}^{SOC}$ is the SOC of the m th MES in time period t. $S_{m,\max}^{SOC}$ and $S_{m,\min}^{SOC}$ are the upper and lower limits of the SOC of the m th MES, respectively.

Eqs. (53)-(57) represent the constraint relationship between the charging and discharging power of the MES and its docking state, charging and discharging flag bits. Eqs. (58) and (59) are the formulas for calculating the SOC of the MES and the upper and lower constraints, respectively.

4.2.3. Distribution network operational constraints. In order to ensure the security of distribution network operation, it needs to satisfy the trend balance constraints, voltage magnitude constraints, DG scheduling constraints, radial topology constraints, and so on, when optimizing the scheduling, as shown below:

1) Tide constraints. The trend calculation model in this chapter follows the linearized trend method [28], which simplifies the form of constraints while ensuring that the solution accuracy meets the requirements:

$$\begin{cases} \sum_{si \in L} P_{si,t} + P_{i,t}^{DG} = P_{i,t}^{Ld} - P_{i,t}^{CL} + P_{i,t}^{d} + \sum_{ij \in L} P_{ij} \\ \sum_{si \in L} Q_{si,t} + Q_{i,t}^{DG} = Q_{i,t}^{Ld} - Q_{i,t}^{CL} + \sum_{ij \in L} Q_{ij,t} \end{cases} \tag{60}$$

$$\begin{cases} U_{i,t}^2 - U_{j,t}^2 \le M(1-b_{ij,t}) + 2(r_{ij}P_{ij,t} + x_{ij}Q_{ij,t}) \\ U_{i,t}^2 - U_{j,t}^2 \ge -M(1-b_{ij,t}) + 2(r_{ij}P_{ij,t} + x_{ij}Q_{ij,t}) \end{cases} \tag{61}$$

$$P_{ij,t}^2 + Q_{ij,t}^2 \le b_{ij,t} S_{ij,\max}^2 \forall ij \in L, t \in T \tag{62}$$

$$\begin{cases} 0 \le P_{i,t}^{CL} \le P_{i,t}^{Ld} \\ Q_{i,t}^{Ld} = P_{i,t}^{Ld} \tan(\cos^{-1}\varphi_i) \forall i \in N, t \in T \\ Q_{i,t}^{CL} = P_{i,t}^{CL} \tan(\cos^{-1}\varphi_i) \end{cases} \tag{63}$$

where L denotes the set of distribution network lines. $P_{y,t}, P_{i,t}^{DG}$ are the active power transmitted by the line between node i, j and the DG active output power at node i in time period t, respectively. $Q_{ij.t}, Q_{i,t}^{po}, Q_{i,t}$ are the reactive power transmitted by the line between node i, j, the DG reactive power and the reactive load demand value at node i in time period t, respectively. $U_{i,t}^2, s_{ij,\max}$ are the squared voltage magnitude at node i and the maximum apparent power value of the line between node ij in time period t, respectively. b_{ij} is a 0-1 variable indicating the connectivity of the line ij in time period t, with 1 for connectivity and 0 otherwise. r_{ij}, x_{ij} denotes the resistance and reactance values of the line ij, respectively. M denotes a constant with a large value. φ_i is the power factor of the load at node i.

Constraint Eq. (60) is the current balance equation considering the cut load and the power consumption of the data center. The line power loss is neglected in constraint equation (61) and this treatment meets the accuracy requirement in the optimization model. Constraint equation (62) indicates that the power circulating on the line must not exceed the allowable value. In this paper the distribution network node loads are treated as controllable loads. Constraint equation (63) indicates that each node load meets the requirement of constant power factor and can be flexibly regulated within the limit of load demand value.

2) DG scheduling constraints:

$$\begin{cases} P_{min}^{DG} \le P_{i,t}^{DG} \le P_{max}^{DG} \\ (P_{i,t}^{DG})^2 + (Q_{i,t}^{DG})^2 \le (S_{max}^{DG})^2 \quad \forall i \in G, t \in T \\ \left| Q_{i,t}^{DG} \right| \le \tan(\cos^{-1}\varphi_{min}^{DG}) P_{i,t}^{DG} \end{cases} \tag{64}$$

where G represents the distribution network DG set. $P_{\min}^{p\alpha}, P_{\max}^{pc}$ represents the minimum active output power and maximum active output power of the DG units at node i, respectively. $S_{\max}^{DG}$ represents the maximum DG apparent power. The constraint equation (64) indicates that the DG active power output must be within the upper and lower power limits, while the active and reactive power outputs must be scheduled under the power factor constraint and capacity constraint limitations.

3) Voltage magnitude constraint:

$$U_{\min^2} \le U_{i,t}^2 \le U_{\max^2} \forall i \in N, t \in T \tag{65}$$

$$\begin{cases} U_r^2 - (1-a_{i,t})M \le U_{i,t}^2 \\ U_r^2 + (1-a_{i,t})M \ge U_{i,t}^2 \end{cases} \forall i \in G, t \in T \tag{66}$$

where, $U_{i,t}^2$ is the square of the voltage magnitude at node i for the t time period. U_r^2 is the distribution network node voltage reference squared. $U_{\min}^2, U_{\max}^2$ are the lower and upper node voltage squared limits, respectively. $a_{i,t}$ is a 0-1 variable indicating whether the DG at t time period node i is the dominant node or not, 1 for yes and 0 otherwise. Constraint equation (66) indicates that the distribution network node voltage magnitude must be within the rated range. Constraint equation (67) indicates that when the DG in the island acts as the dominant power source, it provides voltage support for the loads at the nodes of the island, i.e., the voltage at the DG at this time is the reference voltage.

4) Topological radial constraint. The topological radial constraints are improved, which can make both the energized island and the passive load island satisfy the open-loop structure, and the constraint equation is as follows:

$$\sum_{ij\in L\cup L_v} b_{ij,t} = N_{\text{bus}} - \sum_{i\in G} a_{i,t} \forall t\in T \tag{67}$$

$$F_{i,t}^{DG} + \sum_{si\in L\cup L_v} F_{si,t} = 1 + \sum_{ij\in L\cup L_v} F_{ij,t} \forall t\in T \tag{68}$$

$$\left|F_{ij,t}\right| \le b_{ij,t}\left(N_{bus}+1\right)\forall ij\in L\cup L_v, t\in T \tag{69}$$

$$0\le F_{i,t}^{DG} \le (N_{bus}+1)\forall i\in G_v, t\in T \tag{70}$$

$$0\le F_{i,t}^{DG} \le a_{i,t}(N_{bus}+1)\forall i\in G, t\in T \tag{71}$$

$$a_{i,t} \le k_{i,t} \forall i\in G, t\in T \tag{72}$$

$$k_{i,t} = 0\forall i\in G_v, t\in T \tag{73}$$

$$\left|k_{i,t}-k_{j,t}\right| \le 1-b_{ij,t}\forall ij\in L\cup L_v, t\in T \tag{74}$$

where, L_v denotes the virtual line collection. G_v denotes the set of virtual power sources. N_{bus} denotes the number of distribution network nodes. $F_{i,t}^{DG}$ denotes the virtual power of DG at node i in time slot t. $F_{ij,t}$ denotes the virtual power transmitted on line ij in time slot t. $k_{i,t}$ is a 0-1 variable indicating the charged state of node i in time slot t, with 1 for charged and 0 otherwise. Constraint equation (67) indicates that the radial topology needs to satisfy that the number of bus paths (including virtual lines) is equal to the difference between the number of nodes and the number of islands. Constraint Eq. (68) is the virtual trend balancing constraint, which assumes that the virtual load value at each node is 1. Constraint Eq. (69) restricts the virtual power circulating on each line from exceeding the rated value. Constraints Eqs. (70) and (71) show that the virtual power of a virtual power source is not limited by whether it is the dominant power source or not, and the DG has virtual power only when it is the dominant power source. Constraints (72) and (73) indicate that a virtual power node is not powered and only a powered DG node may be the dominant node. Constraint equation (74) indicates that the connected nodes have the same state of being powered.

4.3. *Model solving*

From the above, it can be seen that the post-disaster power supply restoration optimization model established in this paper is a mixed-integer second-order conic programming problem, which can be solved by invoking a commercial solver.

4.4. *Assessment of indicators*

1) Indicators for assessing post-disaster power supply restoration. In order to reasonably assess the role of the strategy proposed in this paper in the process of post-disaster power supply restoration in distribution networks, four indicators, namely, power loss rate η_z^s, outage economic loss E^s,

response potential E^{DR} and its utilization η^{DR}, are proposed to evaluate the strategy in terms of economy, energy utilization, and power loss profile.

2) The second-order cone relaxation error assessment metrics are shown in Eq. (75):

$$\Delta_{i-j,t} = \left| V_{j,t} I_{i-j,t} - P_{i-j,t}^2 - Q_{i-j,t}^2 \right| \tag{75}$$

where $\Delta_{ij,t}$ is the second-order cone relaxation error at the optimal solution of the model. $P_{i,j,t}$ and $Q_{ij,t}$ are the active and reactive power transmitted by branch $i-j$ in time period t, respectively. $I_{i-j,t}$ and $V_{j,t}$ are the square of the current magnitude flowing through branch $i-j$ and the square of the voltage magnitude at node j at time t, respectively.

5. Example analysis

The disaster recovery strategy proposed in this paper for distribution networks is tested on a modified IEEE-33 node distribution system. The algorithmic analysis is implemented on a computer with an Intel i7-9700 processor and 8 GB of RAM, and the mixed-integer second-order cone planning model is solved using the Gurobi solver in the MATLAB/YALMIP interface.

The improved IEEE-33 node distribution system is shown in Fig. 1, where the critical load nodes are 2, 3, 5, 8, 10, 14, 21, 24, 27, and 30, and the weighting factors for critical and general loads are set to 10 and 1, respectively. Lines 5-6, 9-10, 14-15, 8-21, 9-15, 12-22, 18-33, 25-29 are fitted with remote control switches. The transportation network corresponding to the distribution network is shown in Fig. 2. The correspondence between faulty lines and traffic nodes is shown in Table 1. The test system has 2 repair stations at traffic nodes 6 and 10 of the traffic network, each of which has a repair team at the initial moment, and the repair time of the faulty line is set to 1 hour for each of them.

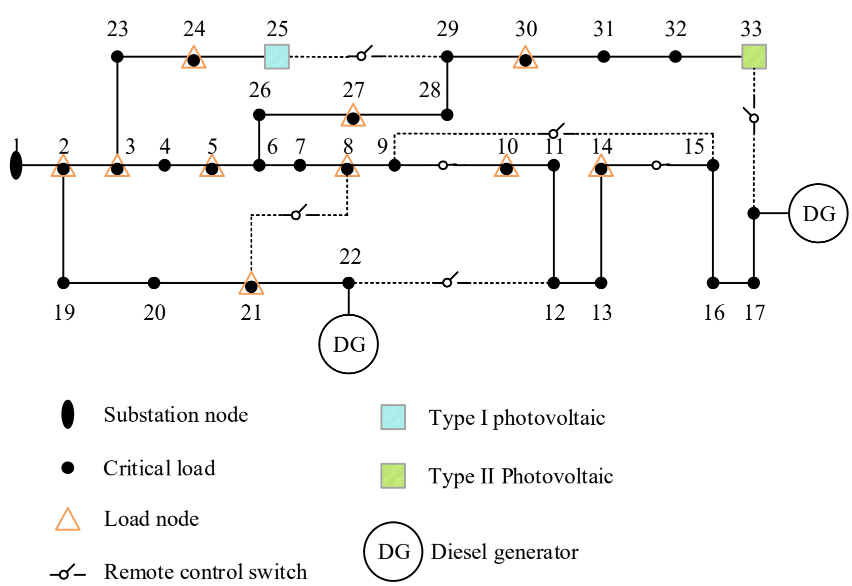

Fig. 1. Improve IEEE-33 node distribution system

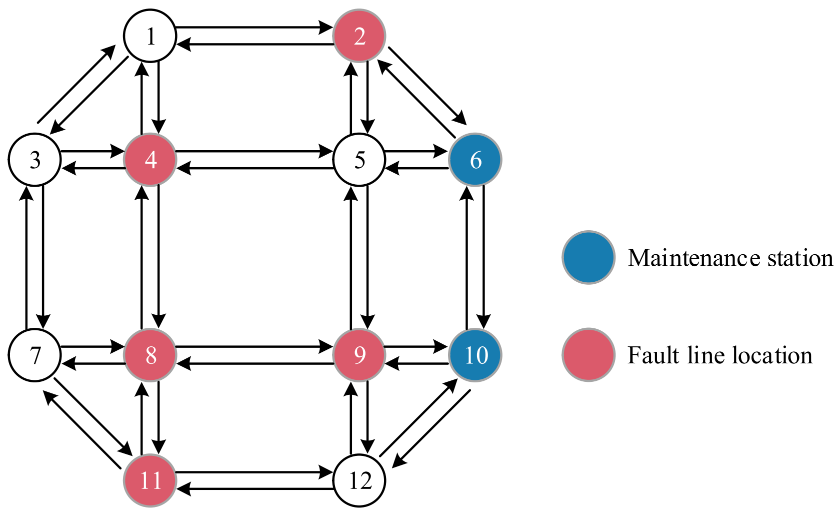

Fig. 2. Traffic network corresponding to the distribution network

Table 1. The corresponding relationship between the failure line and the traffic node

Failure line	2-3	3-4	2-19	3-23	24-25
Traffic node	8	9	11	4	2

In order to verify the effectiveness of the strategy proposed in this paper, six Cases are analyzed in this study:

Case 1: The distribution network is operated and restored according to the strategy proposed in this paper.

Case 2: The distribution network is operated and restored according to the strategy proposed in this paper, but there is no pre-allocation of maintenance teams in the first stage.

Case 3: The distribution network is operated and restored according to the strategy proposed in this paper, but the distribution network contains only the first type of PV systems located at nodes 25 and 33.

Case 4: The distribution network is operated and restored according to the strategy proposed in this paper, but the distribution network does not contain PV and energy storage systems.

Case 5: The distribution network is operated and restored without considering the network loss cost.

Case 6: The distribution network is operated and restored according to the strategy proposed in this paper, but the location of the faulted lines and repair stations on the transportation network is different from Case 1. The faulted lines 2-3, 3-4, 2-19, 3-23, and 24-25 of the distribution network correspond to transportation nodes 7, 10, 12, 3, and 2, and the repair stations are located at transportation nodes 5 and 6.

5.1. Simulation results

This section analyzes the simulation results of the flood disaster recovery strategy for the distribution network, the load recovery of the distribution network is shown in Fig. 3, and the cost of the distribution network under different Cases is shown in Table 2.

From Fig. 3 and Table 2, it can be seen that the load in Case 1 returns to the normal level after 3 hours after the disaster, which is 2 hours faster compared to Case 2. And the total cost in Case 1 is 257080.2 Yuan, which is 72.1% less than the total cost of 919634.7 Yuan in Case 2. This result shows that pre-allocating maintenance teams in Case 1 can enable the distribution network to restore interrupted loads quickly after a fault occurs and reduce the total cost of the distribution network.

At t=4h after the disaster, the load on the distribution grid in Case 1 is 77.3%, which is 7.7% and 26.1% higher compared to Case 3 and Case 4, respectively. Similarly, the total cost of the distribution network in Case 1 is reduced by 16684.2 Yuan and 74493.6 Yuan compared to Case 3 and Case 4. This result indicates that the more variety of flexible resources included in the distribution network, the more resilient the distribution network is against inundation disasters, which reduces the outage losses of the distribution network in case of inundation disasters. In addition, the diversity of flexible resources reduces the total cost of the distribution network.

There is not much difference between the distribution grid loss of load costs in Case 1 and Case 5, but the distribution grid net loss cost in Case 5 is 18,652.2 Yuan higher than that in Case 1, resulting in a higher total cost in Case 5. The reason is that the total cost of the distribution network in Case 5 does not take into account the net loss cost, whose goal is to minimize the outage loss in the event of a failure in the distribution network. However, the increase in the total cost of the distribution network from ignoring the cost of network losses is much greater than the reduction in the total cost from focusing only on the cost of lost loads. Due to the long time interval between the prediction and occurrence of inundation disasters, utilities need to make a trade-off between the cost of network losses and the cost of lost loads so that the total cost of the distribution network is minimized.

Case comparisons for Case 1 and Case 6 are used to illustrate the impact of different traffic constraints on distribution network restoration for transportation networks. For Case 1 and Case 6, different traffic constraints lead to different distribution network load restoration scenarios and total costs. Most of the existing restoration efforts do not consider the traffic constraints of the transportation network during fault restoration, which is not conducive to the utility's scheduling strategy based on the actual traffic conditions.

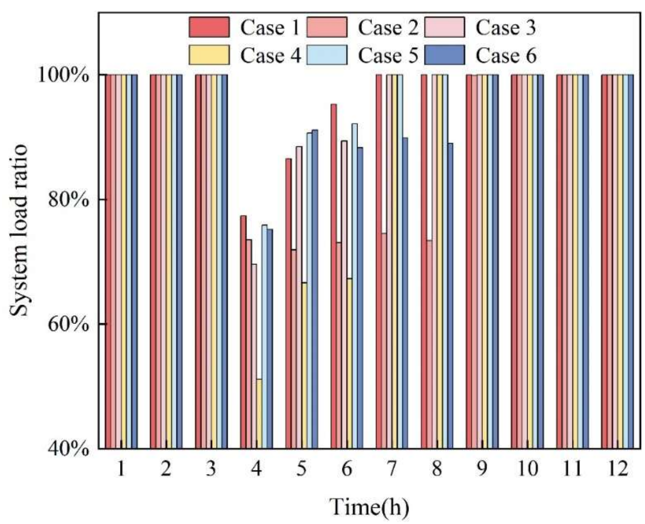

Fig. 3. The load recovery of the distribution network in different cases

Table 2. Distribution cost in different cases (yuan)

Case	Case 1	Case 2	Case 3	Case 4	Case 5	Case 6
Net loss cost	3079.2	3806.7	2596.2	3013.5	21731.4	2477.7
Loss cost	247406.1	903760.2	271270.8	364126.5	247308.6	291739.2
Total cost	257080.2	919634.7	273764.4	331573.8	275227.8	294074.1

The active power of the flexible resources under different Cases is shown in Fig. 4, where the active power over 100% is the network loss of the distribution network and below 0% is the charging of the energy storage system. In the first stage before t=4h, the generator is coupled with the remote remote switch to minimize the network loss of the distribution network and charge the energy storage system before the internal flooding occurs. In the second phase after t=4h, all flexible resources are coordinated with maintenance teams to quickly restore the lost load in the distribution network.

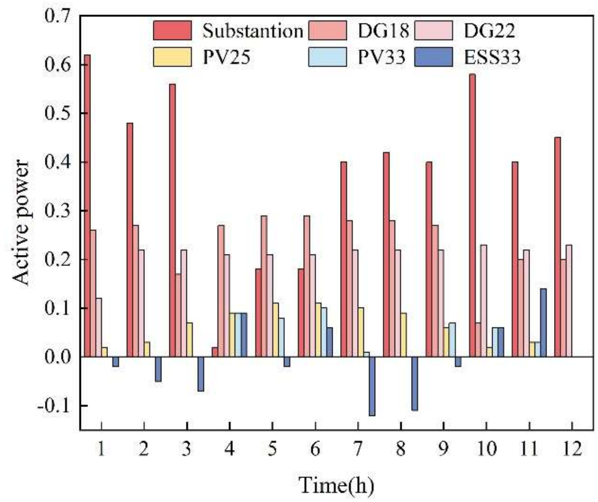

(a) Case 1

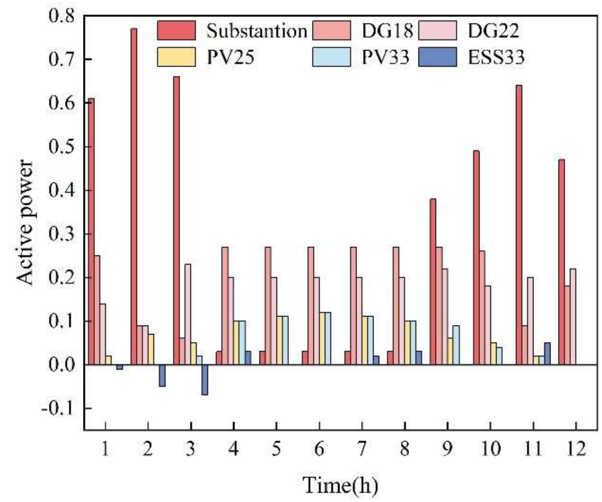

(b) Case 2

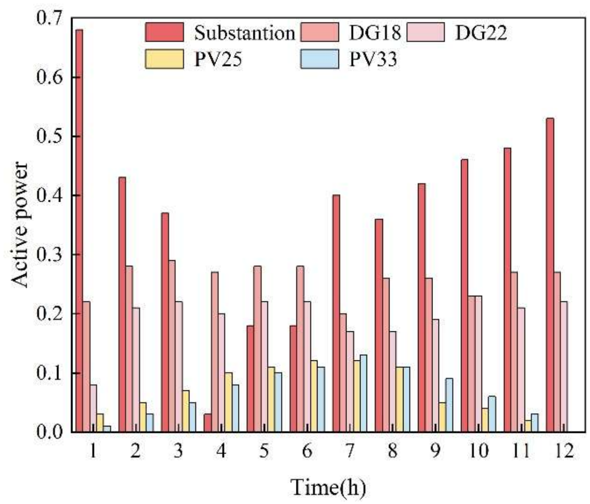

(c) Case 3

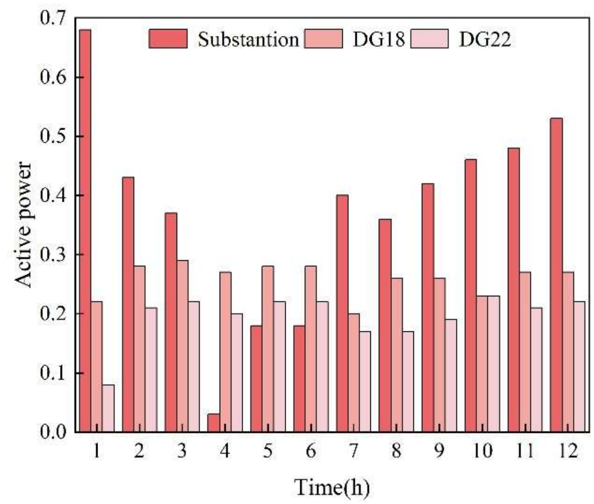

(d) Case 4

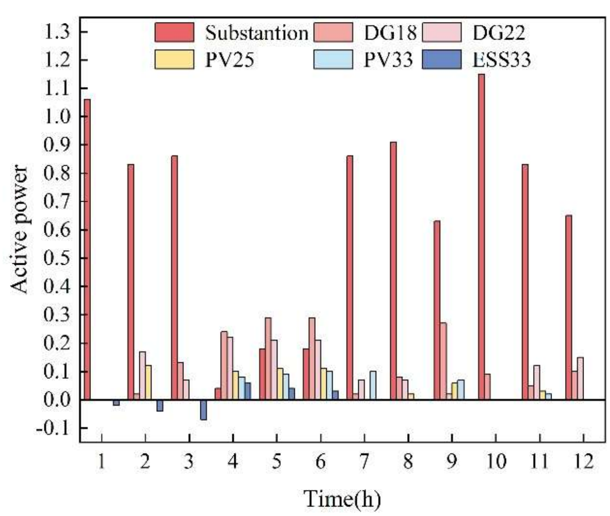

(e) Case 5

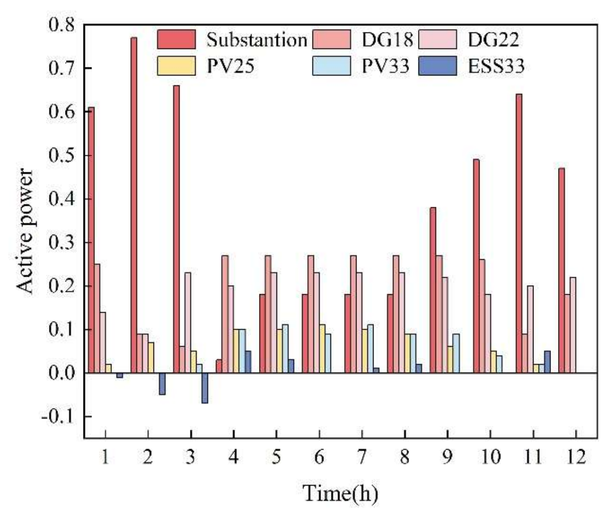

(f) Case 6

Fig. 4. The active power of flexible resources in different cases

The energy changes of the energy storage systems in the four Cases are shown in Fig. 5. In the time period t=1-4h, the energy storage systems in all Cases are charging to cope with the upcoming flooding disaster. At t=4h, the energy storage systems in all Cases start discharging to the distribution grid to maintain power supply to critical loads. After the distribution network is restored to normal, the energy storage systems continue to charge and discharge to minimize the network losses in the distribution network.The energy storage systems in Case 1 can be fully utilized to help the distribution network operation and restoration, which demonstrates the superiority of the strategy proposed in this study.

Due to the different traffic constraints of the transportation network, the scheduling strategies of generators, remote control switches and energy storage systems are different in Case 1 and Case 6. This result shows that the strategy proposed in this paper can develop a reasonable co-dispatch strategy for each flexible resource based on different traffic constraints.

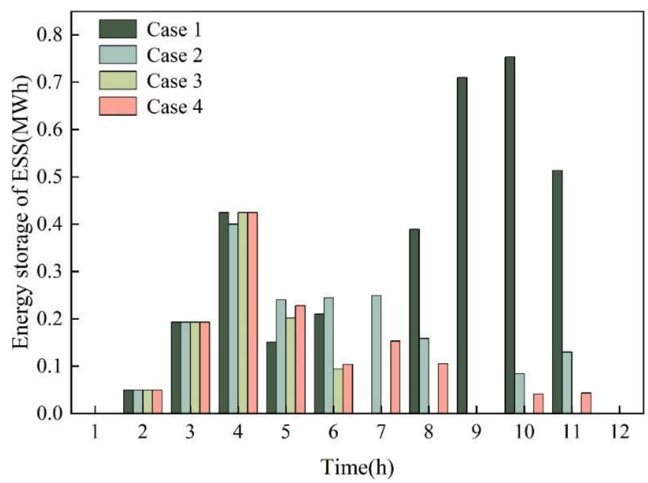

Fig. 5. Energy change of the energy storage system in 4 cases

5.2. Analysis of load restoration and distribution network topology results

5.2.1. Analysis of load recovery results. Case 1 in the IEEE 33-node test system is selected to specifically analyze the results of mobile emergency resource deployment and load restoration.The load restoration of Case 1 is shown in Fig. 6, with (a) and (b) showing the load restoration energy, and weighted load restoration quantity, respectively. Among them, in order to ensure the reliable power supply of important loads in the distribution network, the emergency personnel can carry out sequential scheduling.

From Fig. 6, it can be seen that after the disaster, the repair crew first restores the important paths connecting the primary loads (lines 19-20 and 15-16), and the primary load 21 is restored first, and then the power supply demand of the primary loads 2 and 12 can be satisfied. After completing the repair tasks in the first stage, the repairers make decisions on the next stage of repair tasks based on the load restoration results and limited by the topological constraints of the distribution network, thus restoring more important loads. It should be noted that, due to the limited energy of distributed power sources, under the premise of ensuring reliable and continuous power supply after restoring important loads, it is necessary to ensure the reasonable distribution of energy in the entire time dimension, so the restored loads are all primary loads, and the utilization rate of distributed energy is maximized.

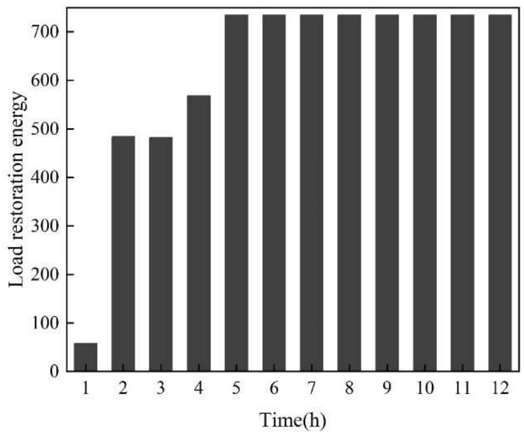

(a) Load restoration energy

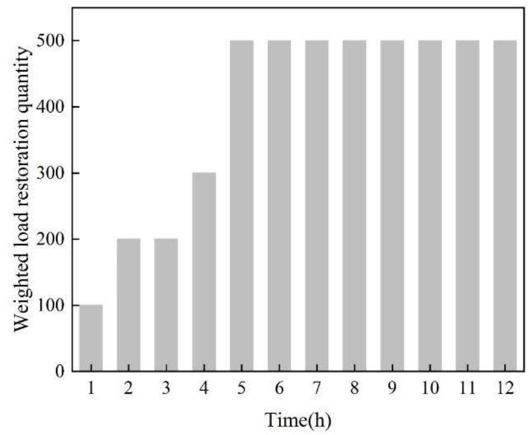

(b) Weighted load restoration quantity

Fig. 6. Load restoration result in each period

5.2.2. Analysis of distribution network topology results. The radial topological constraints proposed in this paper and in the literature are applied in the load recovery model for comparison, respectively, and the number of variables and constraints required for the two different constraints are shown in Table 3. The results show that the two different methods have the same test objective values under 100 scenarios. The computational time required to solve the model under 100 scenarios by applying the different methods is shown in Table 4. It should be noted that in each specific scenario, the solution time of the model applying the topological constraints proposed in this paper is shorter than that of the model applying the constraints proposed in the comparison method.

From the results, it can be seen that the method proposed in this paper is better than the comparison method. As the scale of the test system increases, the superiority of the proposed method becomes more obvious. For the IEEE 123-node test system, the average computation time of the model with constraints is reduced by one order of magnitude compared to the model in the comparison method. The maximum computation time for solving the model with constraints in the comparison method is 1000.54s, which is close to 17min and is not suitable for practical application. In contrast, the maximum solving time of solving the model with constraints based on the constraints proposed in this paper is 38.42s, which is more suitable for online fast decision making.

Table 3. Variables and constraints of two sets of constraints in IEEE 33 and 123-node test systems

Test system	Constraint	Continuous variable	Integer variable	Inequality	Equation
IEEE 33	Our strategy	0	450	850	0
	Contract strategy	450	900	1350	400
IEEE 123	Our strategy	0	1586	3125	0
	Contract strategy	1586	3172	4758	1539

Table 4. Comparison of computation time results

Test system	Solution time	Solution time/s		B/A
		Our strategy (A)	Contract strategy (B)	
IEEE 33	Mean	2.35	20.06	8.54
	Max	30.65	426.74	13.92
	Min	0.14	1.52	10.86
IEEE 123	Mean	2.68	82.65	30.84
	Max	38.42	1000.54	26.04

	Min	0.45	10.32	22.93

5.3. Validation of applicability

In this subsection, a modified IEEE 33-node system is used to verify the applicability of the proposed model in a large distribution system. The restoration power comparison between the proposed model in the paper and the finite cooperative model is shown in Table 5.

The proposed multi-source synergy model is able to restore all the loads within 285 min, which is 45 min faster than the finite synergy model, because the finite synergy model only considers the synergy under the microgrid measure of DG formation, and does not take into account the synergy of the intra-disaster and post-disaster supply paths, which results in some of the class C loads being supplied only by the substation 2 that is delayed in the restoration of power supply, which prolongs the restoration time. In addition, the synergistic model proposed in the paper is able to restore 7,500 kW of load, which is 9.5% more than the limited synergistic model. Meanwhile, in the recovery process of the mid-disaster and post-disaster phases, the proposed multi-source cooperative model restores more load than or equal to the finite cooperative model in the same time. It can be seen that the proposed multi-source cooperative model can not only restore more loads, but also greatly reduce the outage time of loads and improve the speed of load recovery.

Table 5. Total restored power of different schemes in IEEE 33 system

Time/min	Total recovery power/kW	
	Finite cooperative model	Multisource cooperative model
0	0	0
3	325	325
4	325	550
5	1250	1250
6	1250	1800
7	2000	2400
8	2580	2580
110	3250	3250
125	3800	3800
138	4200	4200
149	4200	4450
160	4450	4450
184	4450	4625
199	4850	5000
206	5000	5000
285	5225	7500
330	6850	7500

6. Conclusion

The article constructs a multi-resource cooperative emergency restoration resource scheduling model, proposes a multi-resource cooperative distribution network disaster restoration strategy from two aspects: pre-disaster deployment and post-disaster scheduling, and analyzes the strategy in terms of arithmetic cases.

Among the six Cases, the total cost (257080.2) in Case 1, which is operated and restored in accordance with the strategy proposed in this paper, is the lowest, which is 72.1%, 6.1%, 22.5%, 6.6%, and 12.6% less than the total cost in Case 2, respectively. The maximum, minimum, and average solution time of the proposed multi-source collaborative strategy in this paper are 38.42s, 0.14s, 2.35s (IEEE 33), and 2.68s (IEEE 123), respectively, and the maximum, minimum, and average computation time of the comparison methods are 1000.54s, 1.52s, 20.06s (IEEE 33), and 82.65s (IEEE 123). The multi-source synergy strategy is more suitable for fast decision making. In this paper, the multi-source synergy model is able to recover all the loads within 285min, which is faster than the finite synergy model (45min). The multi-source synergy model is able to restore 7500kW of load, which is 9.5% higher than the finite synergy model. The multi-source synergistic model presents better performance in both load recovery and recovery speed.

Funding

This research was supported by the Science and Technology Project of China Southern Power Grid Company Limited (Project No. 090000KKK52222158).

References

[1] Xiao, Y., Li, B., & Gong, Z. (2018). Real-time identification of urban rainstorm waterlogging disasters based on Weibo big data. Natural Hazards, 94(2), 833-842.

[2] Sun, S., Liu, J., Li, G., Bie, Z., Xu, M., Li, F., & Chen, M. (2023, May). Catastrophe Risk Assessment for Power Distribution Systems under Urban Waterlogging Disasters. In 2023 IEEE 6th International Electrical and Energy Conference (CIEEC) (pp. 3173-3178). IEEE.

[3] Tang, L., Han, Y., Zalhaf, A. S., Zhou, S., Yang, P., Wang, C., & Huang, T. (2024). Resilience enhancement of active distribution networks under extreme disaster scenarios: A comprehensive overview of fault location strategies. Renewable and Sustainable Energy Reviews, 189, 113898.

[4] Chen, B., Ni, M., Yu, C., & Wu, H. (2019, July). Research on Optimizing Recovery Strategy of Distribution Network Communications System in Disaster Based on Mobile Ad-Hoc Networks. In 2019 IEEE 9th Annual International Conference on CYBER Technology in Automation, Control, and Intelligent Systems (CYBER) (pp. 1293-1298). IEEE.

[5] Liu, P., Liu, P., Yang, Y., Wu, J., Tian, G., Zhang, Z., & Chai, L. (2025). Risk Analysis and Mitigation Strategy of Power System Cascading Failure Under the Background of Weather Disaster. Processes, 13(1), 45.

[6] Duan, C., Zhang, J., Chen, Y., Lang, Q., Zhang, Y., Wu, C., & Zhang, Z. (2022). Comprehensive risk assessment of urban waterlogging disaster based on MCDA-GIS integration: The case study of Changchun, China. Remote Sensing, 14(13), 3101.

[7] Du, Y., Liu, Y., Yan, Y., & Jiang, X. (2022). Disaster damage assessment of distribution systems with incomplete and incorrect information. IEEE Transactions on Power Delivery, 38(2), 889-901.

[8] Xia, J., Xu, F., & Huang, G. (2020). Research on power grid resilience and power supply restoration during disasters-A review. Flood Impact Mitigation and Resilience Enhancement, 8.

[9] Moreno, J., & Shaw, D. (2019). Community resilience to power outages after disaster: A case study of the 2010 Chile earthquake and tsunami. International journal of disaster risk reduction, 34, 448-458.

[10] Sun, X., Lin, S., Feng, D., & Zhang, Q. (2024). Post-disaster repair optimization method for traction power supply system of electrified railways based on train operation loss. Reliability Engineering & System Safety, 250, 110301.

[11] Yan, J., Hu, B., Shao, C., Huang, W., Sun, Y., Zhang, W., & Xie, K. (2022). Scheduling post-disaster power system repair with incomplete failure information: A learning-to-rank approach. IEEE Transactions on Power Systems, 37(6), 4630-4641.

[12] Wan, H., Liu, W., Zhang, S., Qie, D., Shi, Q., & Cheng, R. (2025). Pre-disaster allocation and post-disaster dispatch strategies of power emergency resources for resilience enhancement of distribution networks. Electric Power Systems Research, 238, 111038.

[13] Liu, W., Xu, Q., Qin, M., & Yang, Y. (2024). A Post-Disaster Fault Recovery Model for Distribution Networks Considering Road Damage and Dual Repair Teams. Energies, 17(20), 5020.

[14] Liu, W., Zhan, J., Chung, C. Y., & Sun, L. (2019). Availability assessment based case-sensitive power system restoration strategy. IEEE Transactions on Power Systems, 35(2), 1432-1445.

[15] Gao, J., Zhang, Y., Wu, Z., & Yu, L. N. (2025). Optimized collaborative scheduling of unmanned aerial vehicles for emergency material distribution in flood disaster management. Mechatron. Intell Transp. Syst, 4(1), 1-15.

[16] Shigen, G. A. O., Min, Z. H. O. U., Wei, Z. H. E. N. G., Linxuan, Z. H. A. N. G., Bin, Z. H. A. N. G., Haifeng, S. O. N. G., ... & Kunyu, W. A. N. G. (2022). Intelligent operation and maintenance for advanced equipment based on digital twin: Challenges and future. Computer Integrated Manufacturing System, 28(7), 1953.

[17] Xue, Y., Gao, Y., Tian, Y., Liu, H., & Wang, X. (2022). Helicopter rescue for flood disaster: scheduling, simulation, and evaluation. Aerospace, 9(12), 822.

[18] Jiang, J., Li, Q., Wu, L., & Tu, W. (2017). Multi-objective emergency material vehicle dispatching and routing under dynamic constraints in an earthquake disaster environment. ISPRS International Journal of Geo-Information, 6(5), 142.

[19] Zhao, Y., & Zhang, L. (2022). An advanced study of urban emergency medical equipment logistics distribution for different levels of urgency demand. International Journal of Environmental Research and Public Health, 19(18), 11264.

[20] Xia, H., Sun, Z., Wang, Y., Zhang, J. Z., Kamal, M. M., Jasimuddin, S. M., & Islam, N. (2025). Emergency medical supplies scheduling during public health emergencies: algorithm design based on AI techniques. International Journal of Production Research, 63(2), 628-650.

[21] Yan, J., Hu, B., Xie, K., Tai, H. M., & Li, W. (2020). Post-disaster power system restoration planning considering sequence dependent repairing period. International Journal of Electrical Power & Energy Systems, 117, 105612.

[22] Kumar, M. A., & Jaya Laxmi, A. (2018). Power restoration based on intentional islanding algorithm for distributed energy resources in disaster management. International Journal of Modelling and Simulation, 38(3), 189-206.

[23] Moglen, R., Leibowicz, B. D., Kwasinski, A., & Cruse, G. (2024). Optimal restoration of power infrastructure following a disaster with environmental hazards. Socio-Economic Planning Sciences, 101974.

[24] Liu, W., Liu, Y., Yang, Y., Xu, Q., & Dong, F. (2023). Power restoration model for distribution networks after extreme rainstorm disasters based on electric vehicle travel characteristics. Energy Reports, 9, 372-380.

[25] Lu, M., Liu, Y., Yan, Y., Bian, R., Du, Y., & Jiang, X. (2022). Distribution network repair scheduling with multiple types of cooperation using dynamic programming after disasters. IEEE Transactions on Power Delivery, 38(1), 631-641.

[26] San Kim & Sung Kwan Joo. (2025). Spatiotemporal operation method for mobile virtual power line in power system with mobile energy storage systems. Journal of Energy Storage115196-115196.

[27] Hossein Farzin,Fateme Chehrazi & Mohsen Saniei. (2025). Multi-objective planning of mobile energy storage unit in active distribution network considering reliability. Journal of Energy Storage115138-115138.

[28] Seyyedkambiz Mahmoudi,Mohammad Esmail Hamedani Golshan & Pierluigi Siano. (2024). A coordinated voltage control scheme based on linearized power flow functions for non-optimal and optimal problems. Electric Power Systems Research110436-.